# Does Metal Ion Complexation Make Radical Clocks Run Fast?

Anselm H. C. Horn and Timothy Clark*

*Contribution from the Computer-Chemie-Centrum, Friedrich-Alexander-Universität Erlangen-Nürnberg, Nägelsbachstrasse 25, 91052 Erlangen, Germany*

Received July 11, 2002; Revised Manuscript Received October 12, 2002; E-mail: clark@chemie.uni-erlangen.de
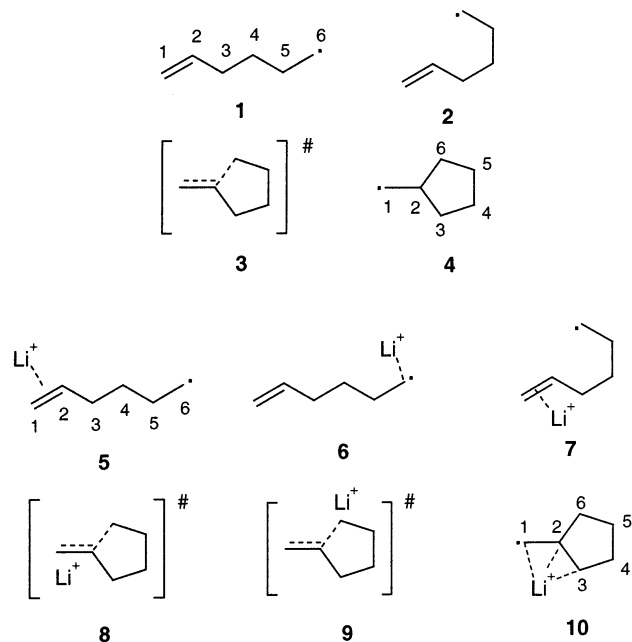
***Abstract:*** Ab initio molecular orbital and density functional calculations at the CBS-RAD(QCISD,B3-LYP) level for $Li^+$ and at B3LYP for $Na^+$, $K^+$, $Cu^+$, and $Ag^+$ reveal that the barrier to ring-closure of the 1-hexen-6-yl ("$\Delta(5)$-hexenyl") radical to the cyclopentylmethyl radical, a so-called radical clock reaction, is decreased very significantly by complexation of the double bond to metal cations. This barrier lowering should occur on complexation with many metal ions, as shown by calculations on all of the monovalent ions listed above. Additional density functional calculations including explicit solvation of the model system complexed to the lithium ion with tetrahydrofuran suggest that the effect found is not limited to the gas phase but may also be significant in experimental radical clock reactions in solution, even for lithium.

## Introduction

Radical clocks[1] are frequently used as a diagnostic tool for detecting radical intermediates in chemical reactions. Briefly, their principle is that an intermediate radical is produced that undergoes a known, fast rearrangement to give characteristic products. As the kinetics of the radical rearrangement are known, those of competing reactions can also be determined from the product distribution. Recently, a new generation of radical clocks that are faster than the classical 1-hexen-6-yl ($\Delta(5)$-hexenyl)[2] has been introduced to be able to study very fast (often biological) reactions.[3]

As the name implies, one of the most important assumptions in the use of radical clocks is that their rearrangement rate is the same under the reaction conditions as that measured in the calibrating kinetic studies. However, we[4] and Radom and co-workers[5] have pointed out the catalytic effect of protonation or metal-ion complexation on many radical reactions. Especially relevant for this case is the calculated acceleration of the methyl radical addition to ethylene by complexation of the latter with $Li^+$.[6] If radical-clock rearrangements are also catalyzed by complexation of the double bond with metal ions, the clocks may run fast under conditions that allow this type of complexation. We have therefore investigated the effect of complexation of the prototype radical-clock rearrangement system (1-hexen-6-yl, **1**, to cyclopentylmethyl, **4**; cf. Chart 1) with a variety of

**Chart 1.** Overview of the Structures Investigated



metal ions using ab initio molecular orbital theory and density functional theory to determine whether such an effect operates.

Radom et al.[7,8] have investigated the performance of different levels of theory for radical reactions in some detail. They conclude that their CBS-RAD technique[9] based on QCISD[10]/6-31G(d)[11] geometry optimizations, B3LYP[12]/6-31G(d) zero-

(1) Griller, D.; Ingold, K. U. *Acc. Chem. Res.* **1980**, *13*, 317.
(2) (a) Brace, N. O. *J. Org. Chem.* **1967**, *32*, 2711. (b) Lal, D.; Griller, D.; Husband, S.; Ingold, K. U. *J. Am. Chem. Soc.* **1974**, *96*, 6355. (c) Schmid, P.; Griller, D.; Ingold, K. U. *Int. J. Chem. Kinet.* **1979**, *11*, 333. (d) Beckwith, A. L. J.; Easton, C. J.; Serelis, A. K. *J. Chem. Soc., Chem. Commun.* **1980**, 482.
(3) Valentine, A. M.; LeTadic-Biadatti, M.-H.; Toy, P. H.; Newcomb, M.; Lippard, S. J. *J. Biol. Chem.* **1999**, *274*, 10771.
(4) Clark, T. *Topics in Current Chemistry, Electron-Transfer II*; Mattay, J., Ed.; Springer-Verlag, Heidelberg, 1996; Vol. 77, p 1.
(5) (a) Golding, B. T.; Radom, L. *J. Chem. Soc., Chem. Commun.* **1973**, 939. (b) Yates, B. F.; Bouma, W. J.; MacLeod, J. K.; Radom, L. *J. Chem. Soc., Chem. Commun.* **1987**, 204.
(6) Clark, T. *J. Chem. Soc., Chem. Commun.* **1986**, 1774.

(7) Wong, M. W.; Radom, L. *J. Phys. Chem.* **1995**, *99*, 8582.
(8) Wong, M. W.; Radom, L. *J. Phys. Chem. A* **1998**, *102*, 2237.
(9) Mayer, P. M.; Parkinson, C. J.; Smith, D. M.; Radom, L. *J. Chem. Phys.* **1998**, *108*, 604, 9598.
(10) Pople, J. A.; Head-Gordon, M.; Raghavachari, K. *J. Chem. Phys.* **1987**, *87*, 5968.
(11) (a) Hehre, W. J.; Ditchfield, R.; Pople, J. A *J. Chem. Phys.* **1980**, *72*, 650. (b) McLean, A. D.; Chandler, G. S. *J. Chem. Phys.* **1980**, *72*, 5639.
(12) Becke, A. D. *J. Chem. Phys.* **1996**, *104*, 1040.

***Table 1.*** Calculated Atom−Atom Distances for the Species **1**−**10**[a]

| distance (Å) | 1 | 2 | 3‡ | 4 | 5 | 6 | 7 | 8‡ | 9‡ | 10 |
|---|---|---|---|---|---|---|---|---|---|---|
| $C_1-C_2$ | 1.334 | 1.334 | 1.370 | 1.489 | 1.355 | 1.335 | 1.357 | 1.386 | 1.382 | 1.493 |
|  | (1.339) | (1.337) | (1.376) | (1.494) | (1.355) | (1.337) | (1.356) | (1.388) | (1.382) | (1.500) |
| $C_5-C_6$ | 1.492 | 1.492 | 1.501 | 1.547 | 1.490 | 1.500 | 1.492 | 1.492 | 1.517 | 1.536 |
|  | (1.496) | (1.497) | (1.505) | (1.542) | (1.497) | (1.504) | (1.498) | (1.500) | (1.519) | (1.532) |
| $C_2-C_6$ | 5.074 | 3.212 | 2.276 | 1.545 | 5.036 | 5.096 | 3.036 | 2.333 | 2.221 | 1.568 |
|  | (5.056) | (2.184) | (2.239) | (1.538) | (5.024) | (5.071) | (3.099) | (2.262) | (2.220) | (1.553) |
| $C_1-C_6$ | 6.083 | 4.295 | 3.014 | 2.564 | 6.002 | 6.045 | 3.977 | 3.064 | 2.910 | 2.546 |
|  | (6.062) | (4.253) | (2.967) | (2.557) | (5.992) | (6.023) | (4.119) | (2.974) | (2.892) | (2.542) |
| $C_1-Li$ |  |  |  |  | 2.223 | 5.075 | 2.209 | 2.145 | 4.965 | 2.212 |
|  |  |  |  |  | (2.294) | (5.052) | (2.280) | (2.196) | (4.973) | (2.254) |
| $C_2-Li$ |  |  |  |  | 2.465 | 4.293 | 2.473 | 2.623 | 4.358 | 2.515 |
|  |  |  |  |  | (2.432) | (4.291) | (2.437) | (2.530) | (4.393) | (2.575) |
| $C_6-Li$ |  |  |  |  | 7.142 | 2.262 | 5.420 | 4.891 | 2.147 | 3.945 |
|  |  |  |  |  | (7.022) | (2.294) | (5.380) | (4.760) | (2.181) | (3.979) |

[a] The first values shown are those calculated at B3LYP/6-31G(d), and those in parentheses are calculated at QCISD/6-31G(d).

point vibrational energies, and CCSD(t)[13] single point energy calculations gives very low errors for the barriers of radical addition reactions to alkenes. We have therefore optimized the all-*trans* conformation of **1**, the conformation that immediately precedes the ring-closure **2**, the product radical **4**, and the cyclization transition state **3** at the QCISD/6-31G(d) and B3LYP/6-31G(d) levels of theory and applied corrections based on further single point energy calculations at higher levels, as outlined by Radom et al.[9] for the CBS-RAD-(QCISD,B3-LYP) procedure. This procedure was used to test the accuracy of B3LYP/6-31G(d) for the uncomplexed reaction and that with Li^{+}. B3LYP/6-31G(d) was then used to investigate the effects of other metals and solvated systems.

## Methods

All calculations used the Gaussian 98 series of programs.[14] Initial optimizations used the Becke three-parameter hybrid technique[12] with the Lee−Yang−Parr correlation functional[15] (B3LYP) with the standard 6-31G(d) basis set.[11] The LanL2DZ basis set[16] was used with standard pseudopotentials and extra polarization functions[17] for copper and silver in combination with 6-31G(d) for carbon and hydrogen. This combination is designated 6-31G(d) in the tables and text. Minima and transition states were confirmed as such by calculation of the normal vibrations at the same level of theory, and the zero-point energies obtained from these calculations were used for the CBS-RAD-(QCISD,B3-LYP) calculations. Further optimizations of the simple systems were also performed using the QCISD technique[10] with the same basis set. Finally, to obtain the CBS-RAD-(QCISD,B3-LYP) energies, the single point energy calculations outlined in Table 5 of the Supporting Information

(13) (a) Purvis, G. D.; Bartlett, R. J. *J. Chem. Phys.* **1982**, *76*, 1910. (b) Raghavachari, K.; Trucks, G. W.; Pople, J. A.; Head-Gordon, M. *Chem. Phys. Lett.* **1989**, *157*, 479.

(14) Frisch, M. J.; Trucks, G. W.; Schlegel, H. B.; Scuseria, G. E.; Robb, M. A.; Cheeseman, J. R.; Zakrzewski, V. G.; Montgomery, J. A., Jr.; Stratmann, R. E.; Burant, J. C.; Dapprich, S.; Millam, J. M.; Daniels, A. D.; Kudin, K. N.; Strain, M. C.; Farkas, O.; Tomasi, J.; Barone, V.; Cossi, M.; Cammi, R.; Mennucci, B.; Pomelli, C.; Adamo, C.; Clifford, S.; Ochterski, J.; Petersson, G. A.; Ayala, P. Y.; Cui, Q.; Morokuma, K.; Rega, N.; Salvador, P.; Dannenberg, J. J.; Malick, D. K.; Rabuck, A. D.; Raghavachari, K.; Foresman, J. B.; Cioslowski, J.; Ortiz, J. V.; Baboul, A. G.; Stefanov, B. B.; Liu, G.; Liashenko, A.; Piskorz, P.; Komaromi, I.; Gomperts, R.; Martin, R. L.; Fox, D. J.; Keith, T.; Al-Laham, M. A.; Peng, C. Y.; Nanayakkara, A.; Challacombe, M.; Gill, P. M. W.; Johnson, B.; Chen, W.; Wong, M. W.; Andres, J. L.; Gonzalez, C.; Head-Gordon, M.; Replogle, E. S.; Pople, J. A. *Gaussian 98*, revision A.11.3; Gaussian, Inc.: Pittsburgh, PA, 2002.

(15) (a) Lee, C.; Yang, W.; Parr, R. G. *Phys. Rev. B* **1988**, *37*, 785. (b) Miehlich, B.; Savin, A.; Stoll, H.; Preuss, H. *Chem. Phys. Lett.* **1989**, *157*, 200.

(16) (a) Hay, P. J.; Wadt, W. R. *J. Chem. Phys.* **1985**, *82*, 270. (b) Wadt, W. R.; Hay, P. J. *J. Chem. Phys.* **1985**, *82*, 284. (c) Hay, P. J.; Wadt, W. R. *J. Chem. Phys.* **1985**, *82*, 299.

(17) Extra polarization functions consisted of one unscaled Gaussian with the following Gaussian exponents α for each function type ("shell"). (a) Cu: p-function, $\alpha_p = 0.117$; f-function, $\alpha_f = 1.440$. (b) Ag: p-function, $\alpha_p = 0.095$; all prefactors were set to 1.0.
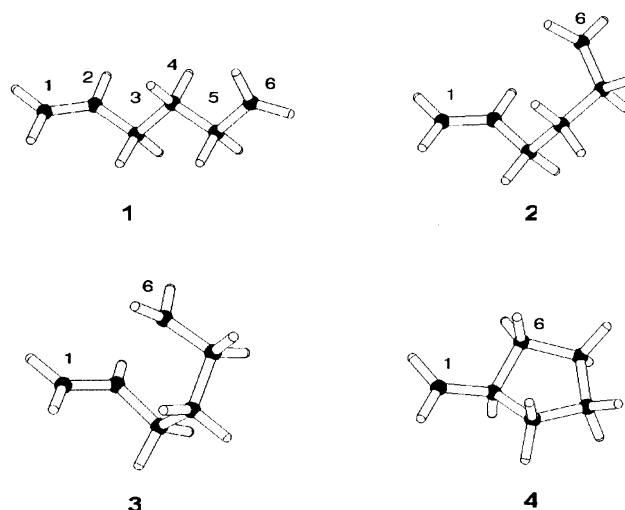
***Figure 1.*** QCISD/6-31G(d) optimized structures of the uncomplexed radical species **1**−**4**. Some geometrical details are given in Table 1.

were performed on the QCISD/6-31G(d) optimized geometries. Unrestricted reference wave functions and DFT techniques were used throughout.

Finally, CBS-RAD-(QCISD,B3-LYP) energies were calculated according to the procedure outlined by Radom and co-workers.[9]

We were unable to locate structures with only real frequencies for some of the systems solvated by tetrahydrofuran molecules (see below). However, the imaginary frequencies (all smaller than 19i cm^{−1}) are within the expected numerical noise of the density functional calculations for systems of this size. Repeated attempts to find "true" minima using the calculated Hessian matrix to start the optimization were unsuccessful.

## Results

**The Parent Reaction.** The QCISD/6-31G(d) optimized geometries of the all-*trans*-1-hexen-6-yl radical, **1**, the precursor conformation for the ring-closing reaction, **2**, the 5-ring-closure transition state, **3**, and the product cyclopentylmethyl radical, **4**, are shown in Figure 1. For comparison, some important bond lengths are compared with those obtained at the B3LYP/6-31G(d) level in Table 1. In general, the agreement between the two calculational methods is good. Table 2 shows the calculated energies for this system, for which several previous computational studies,[18] including a recent comparable one using

(18) (a) Hartung, J.; Stowasser, R.; Vitt, D.; Bringmann, G. *Angew. Chem., Int. Ed. Engl.* **1996**, *35*, 2820. (b) Kemball, M. L.; Walton, J. C.; Ingold, K. U. *J. Chem. Soc., Perkin Trans. 2* **1982**, *8*, 1017.

**Table 2.** Calculated Energies for the Uncomplexed Reaction and That with Li$^{+a}$

| species | QCISD/6-31G(d) | $\langle S^2 \rangle$ | $E_{rel}{}^b$ | B3LYP/6-31G(d) | $\langle S^2 \rangle$ | ZPE | $E_{rel}{}^c$ | CBS-RAD (QCISD, B3-LYP) | $E_{rel}$ |
|---|---|---|---|---|---|---|---|---|---|
| **1** | −234.36798 | 0.763 | 0.0 | −235.17590 | 0.754 | 94.7 | 0.0 | −234.66195 | 0.0 |
| **2** | −234.36567 | 0.793 | 1.4 | −235.17353 | 0.754 | 94.9 | 1.7 | −234.65852 | 2.1 |
| **3‡** | −234.35038 | 1.028 | 11.8 | −235.16217 | 0.786 | 95.5 | 9.4 | −234.64876 | 8.3 |
| **4** | −234.39529 | 0.763 | −17.1 | −235.20055 | 0.754 | 96.9 | −13.3 | −234.68509 | −14.5 |
| **5** | −241.64783 | 0.763 | 0.0 | −242.50854 | 0.754 | 95.8 | 0.0 | −241.93701 | 0.0 |
| **6** | −241.64707 | 0.783 | 0.6 | −242.50713 | 0.753 | 96.3 | 1.4 | −241.93650 | 0.3 |
| **7** | −241.64832 | 0.764 | −0.3 | −242.50892 | 0.754 | 96.1 | −0.1 | −241.93619 | 0.5 |
| **8‡** | −241.63961 | 0.933 | 6.1 | −242.50559 | 0.766 | 96.7 | 2.8 | −241.93194 | 3.2 |
| **9‡** | −241.62747 | 1.003 | 12.9 | −242.49337 | 0.778 | 96.5 | 10.2 | −241.92254 | 9.1 |
| **10** | −241.67846 | 0.761 | −16.3 | −242.53572 | 0.753 | 98.7 | −15.2 | −241.96240 | −15.9 |
| | | | | | | | | | exchange energy$^d$ |
| **Li$^+$(THF)$_4$** | | | | −937.29400 | | 299.6[1]$^e$ | | | 0.0 |
| **5(THF)$_3$** | | | | −940.00097 | 0.754 | 320.5 | 0.0 | | 12.3 |
| **6(THF)$_3$** | | | | −940.00011 | 0.754 | 321.0 | 1.1 | | 11.9 |
| **7(THF)$_3$** | | | | −939.99714 | 0.754 | 320.9 | 2.8 | | 13.6 |
| **8‡(THF)$_3$** | | | | −939.99065 | 0.777 | 321.3 | 7.4 | | 10.2 |
| **9‡(THF)$_3$** | | | | −939.98529 | 0.785 | 321.0 | 10.4 | | 13.2 |
| **10(THF)$_3$** | | | | −940.02567 | 0.753 | 323.0[1]$^f$ | −14.9 | | 12.1 |
| | | | | | | | | | binding energy$^g$ |
| **5(THF)$_4$** | | | | −1172.47281 | 0.754 | 395.2 | 0.0 | | −0.9 |
| **7(THF)$_4$** | | | | −1172.47156 | 0.754 | 395.5 | 1.1 | | −1.5 |
| **8‡(THF)$_4$** | | | | −1172.46126 | 0.782 | 395.7 | 7.7 | | −2.6 |
| **10(THF)$_4$** | | | | −1172.49745 | 0.754 | 397.2 [2]$^h$ | −13.5 | | −1.6 |
| | | | Reference Energies | | | | | | |
| **Li$^+$** | −7.23554 | | | −7.28454 | | | | −7.23584 | |
| **THF** | | | | −232.44929 | | 73.8 | | | |

$^a$ Total energies are given in hartrees; all others are in kcal mol$^{-1}$. Unless noted in square brackets, all minima and transition states are calculated to have the correct number of imaginary frequencies at B3LYP/6-31G(d). $\langle S^2 \rangle$ values for the reference wave functions for the CBS-RAD calculations are given in the Supporting Information. $^b$ QCISD/6-31G(d) relative energies are corrected with unscaled B3LYP/6-31G(d) zero point energies. $^c$ Corrected with unscaled B3LYP/6-31G(d) zero point energies. $^d$ The energy for the displacement of a THF molecule from Li$^+$(THF)$_4$ by the organic radical (B3LYP/6-31G(d) + ZPE). $^e$ The imaginary frequency is calculated to have a frequency of 17i cm$^{-1}$. $^f$ The imaginary frequency is calculated to have a frequency of 13i cm$^{-1}$. $^g$ Complexation energy between the organic radical and Li$^+$(THF)$_4$ (B3LYP/6-31G(d) + ZPE). $^h$ The imaginary frequencies are calculated to have frequencies of −19i and −3i cm$^{-1}$.

theCBS-RAD technique,[19] have been reported. The results of all of the literature studies are consistent, suggesting that calculations on radical-clock reactions are not particularly sensitive to the calculation level.

Our best estimate of the activation energy for this parent reaction is therefore 8.3 kcal mol$^{-1}$ relative to the all-*trans* global minimum **1** and 6.2 kcal mol$^{-1}$ relative to the precursor conformation **2**.

**The Gas-Phase Reaction Complexed to Li$^+$.** We first confirmed that the most stable mode of complexation between **1** and a lithium cation is via the double bond, as assumed in our original study[6] of Li$^+$-catalyzed radical additions to double bonds. We therefore investigated both structures **5**, in which the lithium cation bridges the double bond, and **6**, in which it is complexed directly to the radical center.

We find the double bond complexed isomer **5** to be more stable than the alternative structure at all calculational levels used. Our best estimate (CBS-RAD-(QCISD,B3-LYP)) of the energy difference is 0.3 kcal mol$^{-1}$. Structure **6** is found to be marginally (0.2 kcal mol$^{-1}$) more stable than the double bond complexed precursor conformation **7**, but a radical complexed precursor conformation would be less stable. Figure 2 shows the optimized structures. The calculated energies for the Li$^+$ complexed structures in the gas phase are shown in Table 2. Although the relative energies are so close that we cannot definitively assign a most stable conformer for **5**–**7**, the
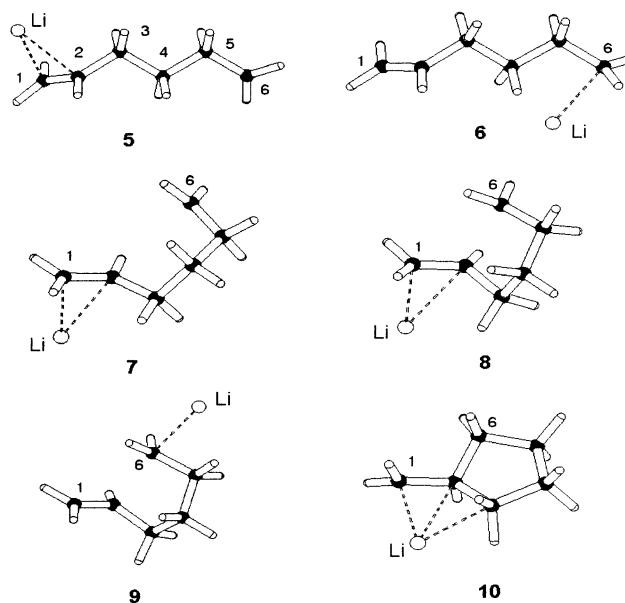
(19) Maxwell, B. J.; Smith, B. J.; Tsanaktsidis, J. *J. Chem. Soc., Perkin Trans. 2* **2000**, *3*, 425.



**Figure 2.** QCISD/6-31G(d) optimized structures of the Li$^+$ complexed radical species **5**–**10**. Some geometrical details are given in Table 1. The dashed lines connecting the radical system to the cation are based only on the contact distances and do not imply a covalent bonding interaction.

calculated stabilities seem intuitively reasonable. However, the three conformations are likely to coexist in equilibrium.

The CBS-RAD complexation energies between the lithium cation and the radical species are −24.6, −24.3, −26.3, −29.7, −23.8, and −26.0 kcal mol$^{-1}$ for **5**–**10**, respectively. Thus, the cation complexes most strongly to the transition state **8‡** and

***Table 3.*** Calculated Energies for the $Na^+$, $K^+$, $Cu^+$, and $Ag^+$ Complexed Systems[a]

| | | B3LYP/6-31G(d) | | | | $E_{rel}$ | |
| --- | --- | --- | --- | --- | --- | --- | --- |
| | NIMAG | Na | $\langle S^2 \rangle$ | K | $\langle S^2 \rangle$ | Na | K |
| **5-M** | 0 | −397.29119, (95.5) | 0.754 | −834.92145, (95.3) | 0.754 | 0.0 | 0.0 |
| **6-M** | 0 | −397.28937, (95.8) | 0.753 | −834.91954, (95.7) | 0.753 | 0.8 | 1.6 |
| **7-M** | 0 | −397.29120, (95.8) | 0.754 | −834.92103, (95.6) | 0.754 | 0.3 | 0.6 |
| **8-M‡** | 1 | −397.28580, (96.4) | 0.769 | −834.91311, (96.1) | 0.774 | 4.3 | 6.0 |
| **10-M** | 0 | −397.31665, (98.2) | 0.754 | −834.94665, (98.0) | 0.754 | −13.3 | −13.1 |
| | | Cu | | Ag | | Cu | Ag |
| **5-M** | 0 | −431.09498, (96.0) | 0.755 | −380.71655, (96.0) | 0.755 | 0.0 | 0.0 |
| **6-M** | 0 | −431.08786, (96.1) | 0.759 | −380.71014, (96.3) | 0.761 | 4.6 | 4.3 |
| **7-M** | 0 | −431.09178, (95.8) | 0.754 | −380.71331, (95.9) | 0.755 | 1.8 | 1.9 |
| **8-M‡** | 1 | −431.08828, (96.7) | 0.754 | −380.70879, (95.8) | 0.754 | 4.9 | 4.7 |
| **10-M** | 0 | −431.11537, (98.4) | 0.757 | −380.73902, (98.6) | 0.755 | −10.4 | −11.5 |

[a] Total energies are given in hartrees; zero point energies (in parentheses) and relative energies are in kcal mol$^{-1}$. Details of the basis set and pseudopotentials used for Cu and Ag are given in the Methods section. NIMAG is the number of imaginary frequencies.

slightly more strongly to the double bond in **7**, in which an interaction between the radical center and the double bond already exists as compared to in either the all-*trans* conformation **5** or the radical complexed isomer **6**. Moreover, complexation with the lithium cation does not change the overall thermodynamics of the reaction (**5** and **10** have similar complexation energies), as was also found in our earlier study on methyl radical addition to ethylene.[6] However, **10** shows some geometrical evidence for an agostic stabilization between the lithium cation and an adjacent $CH_2$ group that may only be relevant in the unsolvated species (however, see below).

Although **5** is clearly the more stable complex between $Li^+$ and the 1-hexen-6-yl radical, we located the 5-ring-closure transition states arising from both **5** and **6** to rule out a kinetic preference for ring-closure of the less stable complex. The two transition states thus obtained (**8‡** and **9‡**) are also shown in Figure 2.

As found for complexes **5** and **6**, the double bond complexed isomer **8‡** is more stable than the radical complexed structure **9‡**. Thus, both the more stable complex and the more stable ring-closure transition state correspond to the double bond complexed structures investigated in our original work.[4]

The geometry changes that occur in the organic radical upon lithium cation complexation are relatively minor. Perhaps the most significant changes are those in the double bond ($C_1-C_2$) length in all complexes and in the $C_2-C_6$ distance (forming $C-C$ bond) in the transition states. The double bond is lengthened by roughly 0.02 Å relative to the unperturbed species in all structures in which it is directly complexed to the metal ion. The forming $C-C$ bond in the $Li^+$ complexed transition state **8‡** (2.262 Å) is shorter than that in the unperturbed transition state **3‡** (2.239 Å), but that in **9‡** (2.220 Å) is shorter. In the double bond complexed species **5**, **7**, and **8‡**, the lithium cation bridges the alkene bond unsymmetrically. In all cases, it is closer to $C_1$ than to $C_2$. The radical complexed structures **6** and **9‡** exhibit classical $C-Li$ one-electron-bonded structures. The product radical **10** shows this type of bonding as well as agostic interactions between the metal ion and the hydrogens of the $C_3$-methylene. Interestingly, the $C_2-C_6$ bond opposite of the metal is also lengthened significantly.

The calculated energies for the gas-phase lithium cation complexed reaction are shown in Table 2. The activation energy is reduced significantly by $Li^+$-complexation to a CBS-RAD-(QCISD,B3-LYP) value of only 3.2 kcal mol$^{-1}$ relative to the

most stable complex calculated, **5**, and 2.7 kcal mol$^{-1}$ relative to the immediate precursor complex **7**. Interestingly, **2** is stabilized by 1.8 kcal mol$^{-1}$ relative to **1** by lithium complexation, presumably because the nascent three-electron interaction between the radical center and the double bond enjoys some electrostatic stabilization.[4,20] However, complexation of the metal to the radical center increases the activation energy slightly (from 8.3 to 9.1 kcal mol$^{-1}$) relative to the uncomplexed reaction.

**Complexes with Other Metal Cations.** In view of the reasonable agreement shown in Table 2 between B3LYP/6-31G(d) and the CBS-RAD-(QCISD,B3-LYP) values, calculations with other monovalent metal ions were performed at the density functional level of theory. The calculated energies are shown in Table 3, and some relevant geometrical parameters are shown in Table 4.

The alkali metal ions behave exactly as expected on the grounds of their sizes. The stabilization of the precursor conformation **7** relative to the all-*trans* complex **5** and the lowering of the cyclization barrier decrease with increasing cation size. The heat of reaction is affected little by complexation to the different metals. However, all three metals are calculated to lower the cyclization barrier significantly with respect to the uncomplexed system **5**. The geometries of the alkali metal complexes show exactly the same trends, attenuated by the cation size, as described above for $Li^+$.

The monovalent transition metal ions $Cu^+$ and $Ag^+$ behave slightly differently, as might be expected from the fact that they can enter into additional covalent interactions not available to the alkali metal ions. $Cu^+$ and $Ag^+$ show a far stronger preference (4−5 kcal mol$^{-1}$) for the double bond complexed structure **5** over its radical complexed equivalent **6**. This might be expected from the experimentally known[21] affinity of copper-(I) and especially silver(I) for alkenes. This strong bonding also occurs at the expense of the three-electron interaction between the radical center and the double bond in **7**, which is found to be almost 2 kcal mol$^{-1}$ less stable than **5** for the $Cu^+$ and $Ag^+$ complexes. These values are close to that found for the

(20) Clark, T. *J. Am. Chem. Soc.* **1988**, *110*, 1672.
(21) (a) Kochi, J. K. *J. Organomet. Chem.* **1972**, *43*, C7−C10. (b) Natarajan, G. S.; Venkatachalam, K. A.; Laxminarayan, *J. Inst. Eng. (India, Part CH)* **1976**, *56*, 94. (c) Natarajan, G. S.; Venkatachalam, K. A. *Aust. J. Chem.* **1974**, *27*, 1209. (d) Salomon, R. G.; De Ligny, C. L.; Van T Verlaat, T.; Karthaus, F. *J. Chromatogr.* **1973**, *76*, 115. Rothberg, I.; Krieg, W. J.; Sisco, W. R. *J. Org. Chem.* **1971**, *36*, 4076.

**Table 4.** Calculated (B3LYP/6-31G(d)) Atom−Atom Distances for the $Na^+$, $K^+$, $Cu^+$, and $Ag^+$ Complexed Systems[a]

| distance (Å) | 5-Na | 6-Na | 7-Na | 8-Na‡ | 10-Na | 5-K | 6-K | 7-K | 8-K‡ | 10-K |
|---|---|---|---|---|---|---|---|---|---|---|
| $C_1-C_2$ | 1.351 | 1.335 | 1.352 | 1.405 | 1.489 | 1.345 | 1.334 | 1.345 | 1.405 | 1.489 |
| $C_5-C_6$ | 1.491 | 1.495 | 1.493 | 1.498 | | 1.491 | 1.495 | 1.493 | 1.498 | |
| $C_2-C_6$ | 5.047 | 5.081 | 3.114 | 2.156 | 1.566 | 5.063 | 5.087 | 3.161 | 2.156 | 1.565 |
| $C_1-C_6$ | 6.005 | 6.053 | 4.117 | 2.898 | 1.563 | 6.047 | 6.001 | 4.217 | 2.898 | 1.561 |
| $C_1-M$ | 2.579 | 5.367 | 2.569 | 2.500 | 2.581 | 3.094 | 5.853 | 3.070 | 2.500 | 3.032 |
| $C_2-M$ | 2.790 | 4.661 | 2.785 | 2.967 | 3.003 | 3.230 | 5.055 | 3.252 | 2.967 | 3.525 |
| $C_6-M$ | 7.433 | 2.640 | 5.723 | 5.074 | | 7.688 | 3.112 | 6.126 | 5.074 | |
| $C_3-M$ | | | | | 2.740 | | | | | 3.313 |

| distance (Å) | 5-Cu | 6-Cu | 7-Cu | 8-Cu‡ | 10-Cu | 5-Ag | 6-Ag | 7-Ag | 8-Ag‡ | 10-Ag |
|---|---|---|---|---|---|---|---|---|---|---|
| $C_1-C_2$ | 1.386 | 1.344 | 1.384 | 1.383 | 1.488 | 1.379 | 1.344 | 1.377 | 1.376 | 1.469 |
| $C_5-C_6$ | 1.484 | 1.500 | 1.489 | 1.494 | | 1.483 | 1.487 | 1.487 | 1.490 | |
| $C_2-C_6$ | 5.000 | 5.074 | 4.478 | 3.324 | 1.573 | 5.001 | 5.075 | 4.469 | 3.977 | 1.605 |
| $C_1-C_6$ | 5.907 | 5.960 | 5.423 | 4.250 | 1.562 | 5.910 | 5.944 | 5.405 | 4.973 | 1.554 |
| $C_1-M$ | 2.050 | 5.639 | 2.057 | 2.063 | 2.027 | 2.312 | 6.179 | 2.321 | 2.322 | 2.304 |
| $C_2-M$ | 2.296 | 4.755 | 2.280 | 2.265 | 2.593 | 2.623 | 5.263 | 2.608 | 2.584 | 3.050 |
| $C_6-M$ | 7.066 | 2.013 | 6.731 | 5.509 | | 7.378 | 2.309 | 7.050 | 6.480 | |
| $C_3-M$ | | | | | 2.578 | | | | | 3.392 |

[a] Details of the basis set and pseudopotentials used for Cu and Ag are given in the Methods section.

uncomplexed radical. As a consequence of the weakening of the three-electron interaction, **7-Cu** and **7-Ag** adopt more open conformations than **7-Li**, **7-Na**, and **7-K**. The radical centers point away from the double bond, and the $C_2-C_6$ distances in the two transition metal ion complexes are therefore increased from about 3.2 Å for the alkali metals to around 4.5 Å for copper and silver.

The activation energies for the cyclization reaction are also lowered to about one-half of the value found for the uncomplexed reaction by $Cu^+$ and $Ag^+$. However, the transition states occur much earlier than either the uncomplexed or the alkali-metal ion catalyzed reactions. The lengths of the forming ($C_2-C_6$) C−C bonds are 3.324 and 3.977 Å in **8-Cu‡** and **8-Ag‡**, respectively. Because of the strong complexation to the double bond in the reactant radicals, the overall reactions are from 1.6 to 5.5 kcal mol$^{-1}$ less exothermic than the uncomplexed or the alkali metal ion complexed reactions.

**Model Solvation Calculations.** Reactions involving metal cations seldom happen in vacuo.[22] It is therefore important to consider the possible effect of donor solvents that might destroy the effect found above for the gas phase. We have thus calculated the model reaction with a supermolecule approach in which we have solvated the lithium cation with three or four molecules of tetrahydrofuran. The lithium cation is known[23] to form a complex with four THF molecules. We have used a supermolecule approach rather than the more economical polarizable continuum model alternative to be able to treat specific solvent−cation interactions adequately. Structures **5**, **6**, **7**, **8‡**, **9‡**, and **10** were extended by adding three coordinating THF molecules to the cation to give **5(THF)₃** etc. Figure 3 shows the optimized structures graphically; details of their geometries are given in the Supporting Information.

Table 2 shows the energies obtained for structures with the radical species complexed to $Li^+(THF)_3$ and for the $Li^+(THF)_4$ complex. As expected, none of the radical structures are able to displace THF from $Li^+(THF)_4$, as shown by the calculated exchange energies in Table 2, which range from 10 to 14 kcal mol$^{-1}$. Complexation of the lithium cation with three THF

molecules also weakens the preferential electrostatic stabilization of the cyclization transition state relevant to the reactant and product, but a diminished effect is still found. The calculated activation energy relative to **5(THF)₃** is 7.4 kcal mol$^{-1}$, as compared with 2.8 for the reaction complexed to the "naked" lithium cation and 9.4 for the parent, uncatalyzed reaction.

A second series of calculations on the THF-solvated lithium cation systems were performed in which the radical partner complexes additionally to $Li^+(THF)_4$, rather than to displace one of the THF ligands from the cation. The geometries obtained are shown in Figure 4, and details are given in the Supporting Information.

This situation is a more realistic representation of the situation in solution, at least for the alkali-metal cations. In this case, the structures considered all bind weakly to $Li^+(THF)_4$, with binding energies from 0.9 to 2.6 kcal mol$^{-1}$, but a moderated preference for the transition state is still observed, with an activation energy relative to **5(THF)₄** of 7.7 kcal mol$^{-1}$, very similar to that found for the system with only three THF molecules. This effect is found despite the fact that the Li−radical distance increases to 4.5−5.3 Å in the $Li^+(THF)_4$ complexed systems. These results are consistent with the essentially electrostatic nature of the catalysis,[4] as the catalytic effect decreases with increasing distance from the charged center and does not require a direct covalent interaction with the metal ion.

## Discussion

The gas-phase calculations demonstrate convincingly the barrier-lowering effect of complexation of the 1-hexen-6-yl radical with a lithium cation. The barrier lowering from 8.3 to 3.2 kcal mol$^{-1}$ (CBS-RAD-(QCISD,B3LYP), relative to the all-*trans* conformation of the radical) for the lithium cation corresponds to a rate acceleration by a factor of 5200 if we assume a constant preexponential factor at room temperature. Thus, there can be little doubt that complexation of the 1-hexen-6-yl radical with a metal cation in vacuo should provide an enormous acceleration of the ring-closure reaction to give cyclopentylmethyl. This acceleration can be attributed to the electrostatic effect of the complexing ion on the odd-electron bonding that is most important in the transition states of radical reactions.[4,20] Are the gas-phase results, however, at all relevant for "real" reaction conditions?

(22) See, however: (a) Schroeder, D.; Heinemann, C.; Koch, W.; Schwarz, H. *Pure Appl. Chem.* **1997**, *69*, 273. (b) Schroeder, D.; Schwarz, H. *Angew. Chem., Int. Ed. Engl.* **1995**, *34*, 1973.
(23) Orpen, G. A.; Quayle, M. J. *J. Chem. Soc., Dalton Trans.* **2001**, 1601.
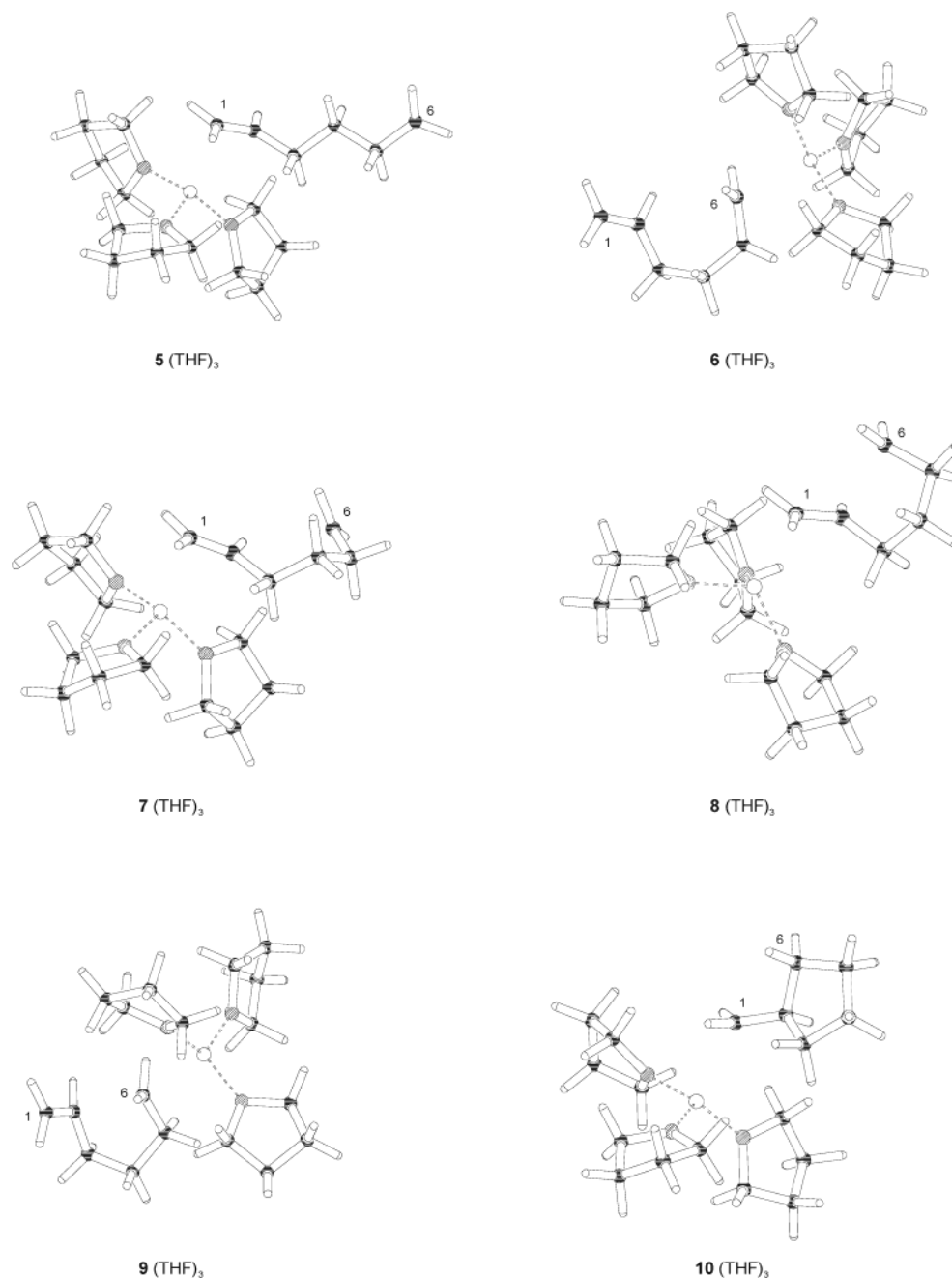
**5** (THF)$_3$

**6** (THF)$_3$

**7** (THF)$_3$

**8** (THF)$_3$

**9** (THF)$_3$

**10** (THF)$_3$

***Figure 3.*** B3LYP/6-31G(d) optimized structures of the Li$^+$ complexed species coordinated to three THF molecules. Details are given in the Supporting Information. The dashed lines connecting the radical system to the cation are based only on the contact distances and do not imply a covalent bonding interaction.

There is ample evidence in the literature of copper(I) and silver(I) ions complexing strongly with alkenes.[21] Indeed, the latter are often used in separation techniques involving alkenes.[24] It is, however, much more questionable whether the alkali ions can affect the kinetics of radical clock reactions in typical donor solvents. The calculated exchange reactions shown in Table 2 suggest that isolated THF-solvated lithium ions will not complex a hexenyl radical at the expense of a THF ligand, as expected. The interaction between a radical and a fully solvated lithium cation is weak (2–3 kcal mol$^{-1}$), but the resulting complex does show a small (1.7 kcal mol$^{-1}$) lowering of the cyclization barrier that would be significant kinetically (it would result in a roughly

18-fold increase in the rate). Can there, however, be special situations, such as aggregation, that favor complexation of C= C double bonds to alkali metal ions? Entropic factors, which are beyond the scope of this investigation, may also be significant for cyclization reactions. The entropic effect of metal-ion complexation, however, can probably best be described as a preorganization of the correct conformation for cyclization (by strengthening the nascent odd-electron interaction between the double bond and the radical center), so that, if anything, we expect metal-ion coordination to result in an entropic acceleration of the reaction.

The closest analogies that we have been able to find in the literature are X-ray structures in which sodium ions are complexed to C=C double bonds in [(allyl)$_2$Si(C$_5$H$_4$)$_2$Na]$^-$ [25]

(24) See, for instance: Thoen, P. M.; Noble, R. D.; Koval, C. A. *J. Phys. Chem.* **1994**, *98*, 1262.

Li(THF)$_4$

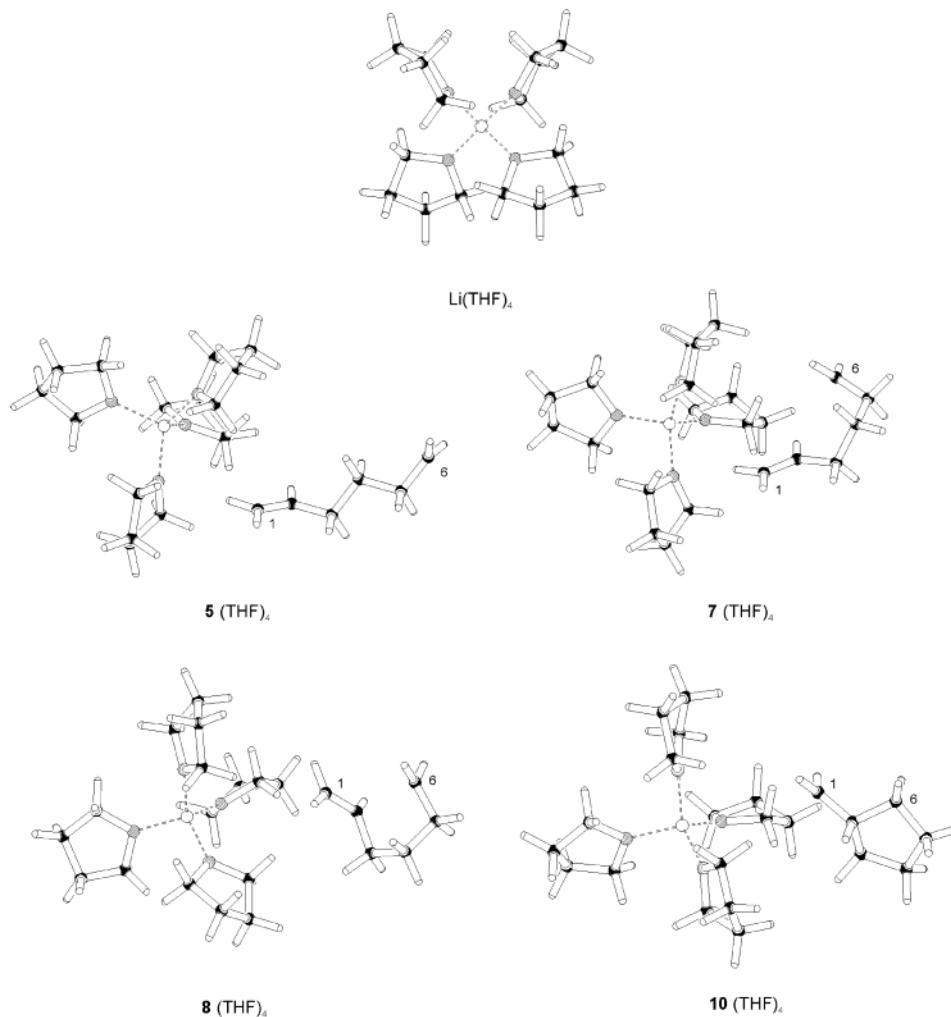5 (THF)$_4$       7 (THF)$_4$

8 (THF)$_4$       10 (THF)$_4$

***Figure 4.*** B3LYP/6-31G(d) optimized structures of the Li$^+$ complexed species coordinated to four THF molecules. Details are given in the Supporting Information. The dashed lines connecting the radical system to the cation are based only on the contact distances and do not imply a covalent bonding interaction.

and in a more recent example with a lariat crown ether.[26] In this compound, the sodium ion is $\pi$-complexed to two C=C bonds, although it is also coordinated to four ether oxygens and two tertiary amine donors from the ether ring. It is also known that olefins complex quite strongly to Na$^+$ within zeolites.[27] Thus, the experimental evidence suggests that sodium, and probably also lithium, can complex to carbon–carbon double bonds even in solution in donor solvents.

The catalysis that we have found shows all of the characteristics of a purely electrostatic effect for the alkali metal ions. This can be demonstrated by plotting the calculated activation energy for the cyclization against the C$_1$–metal distance, as shown in Figure 5. The solid line and the circular points give the activation energy relative to **5** and the triangles and dashed line relative to **7**. The alkali metals are represented by black symbols, and the transition metals are represented by open symbols.

The three alkali metals show a linear relationship between the activation energy and the ion–ligand distance. This may,
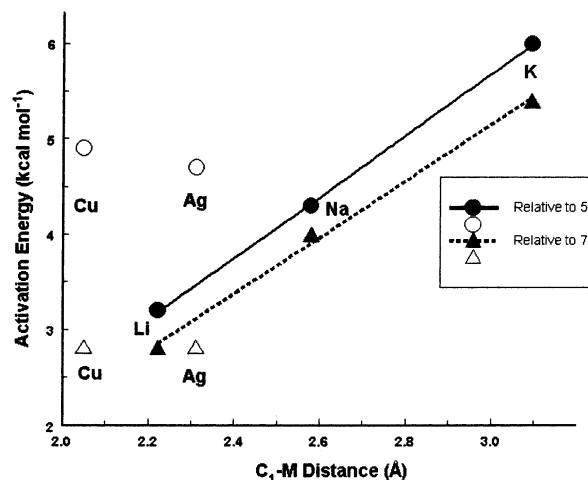


***Figure 5.*** Plot of the calculated activation energies against the C–metal distances. The alkali metals are shown as black symbols; the transition metals are shown as their open equivalents.

in fact, be reciprocal as might be expected from Coulomb's law, but the data do not justify any conclusions in this respect. We limit our conclusions to the observation that the lowering of the activation energy is directly connected to the distance

(25) Harder, S.; Lutz, M.; Obert, S. J. *Organometallics* **1999**, *18*, 1808.
(26) Hu, J.; Barbour, L. J.; Gokel, G. W. *Chem. Commun.* **2001**, 1858.
(27) Herden, H.; Meiler, W.; Robien, W. *Monatsh. Chem.* **1988**, *119*, 913. Sauer, J.; Deininger, D. *Zeolites* **1982**, *2*, 114.

between the alkali metal ions and the reacting system, as would be expected of purely electrostatic catalysis. The two transition metals show lower barriers relative to **5** than would be expected from their size. This is not the case relative to **7** because of the preferential stabilization of **5** by copper(I) and silver(I). Figure 4 suggests, however, that the transition metals can interact covalently with the radical system in addition to their electrostatic effect.

## Conclusions

The effect that we have described above may or may not be important in experimental studies. However, we believe that possible rate accelerations of up to a factor of $10^4$ in radical clock reactions because of the presence of metal ions in solution should be considered and that it is necessary to test the proposed effect on a suitable experimental system. This is especially true in light of the many studies that have used radical clocks either in organometallic reaction systems or in the active sites of metalloenzymes. We also note that our earlier calculations on other open-shell reactions suggested that strong electrostatic fields, such as those encountered in, for instance, zeolites or enzyme active sites, are also capable of lowering activation energies significantly.[28]

**Supporting Information Available:** Tables detailing the single point calculations performed and giving detailed CBS-RAD (QCISD, B3-LYP) energy contributions of structures **1**−**10** (PDF); Gaussian archive entries of all structures investigated (**1**−**10**, **5-M**−**10-M**) (ASCII). This material is available free of charge via the Internet at http://pubs.acs.org.

JA020954K

(28) Hofmann, H. Ph.D. Thesis, Universität Erlangen-Nürnberg, 1992.